Temporal and spatial scales of sea-surface temperature variability in Canadian Atlantic waters

M. Ouellet, B. Petrie and J. Chassé

Ocean Sciences Division
Maritimes Region
Fisheries and Oceans Canada

Bedford Institute of Oceanography
P.O. Box 1006
Dartmouth, Nova Scotia
Canada B2Y 4A2

2003

Canadian Technical Report of Hydrography and Ocean Sciences 228

Fisheries and Oceans Canada | Pêches et Océans Canada

Canada

103-03580/

Canadian Technical Report of
Hydrography and Ocean Sciences 228

2003

Temporal and spatial scales of sea-surface temperature variability in Canadian Atlantic waters

by

M. Ouellet, B. Petrie and J. Chassé

Ocean Sciences Division
Maritimes Region
Department of Fisheries and Oceans
Bedford Institute of Oceanography
P.O. Box 1006
Dartmouth, Nova Scotia
Canada B2Y 4A2

© Her Majesty the Queen in Right of Canada 2003
Cat. No. Fs 97-18/228E ISSN 0711-6764

Correct citation for this publication :

Ouellet, M., B. Petrie and J. Chassé. 2003. Temporal and spatial scales of sea-surface temperature variability in Canadian Atlantic waters. Can. Tech. Rep. Hydrogr. Ocean Sci. 228: v + 30 p.

TABLE OF CONTENTS

Table of Contents iii
List of Figures iii
List of Tables iv
Abstract/Résumé v
1.Introduction 1
2.Data and Methods 1
2.1 Data 1
2.2 Harmonic analysis and SST anomalies 1
2.3 Calculation of correlation coefficients 2
3.Results 3
3.1 Harmonic analysis 3
3.2 Temporal scales of variability 5
3.3 Spatial coherence scales of variability 6
3.4 Spatial coherence scales of variability at different sampling frequencies 7
4.Conclusion 7
5.Acknowledgements 8
6.References 8
Appendix I 30

LIST OF FIGURES

Figure 1. Names and locations of places mentioned in the text and locations (red pixels) where neighbour averaging was necessary to extract the harmonic signal. 13
Figure 2. Percentage of total variance of the SST accounted for by the harmonic fit (the dotted line is the 200 m isobath, the thick white line is the shelf-slope front mean position and the thin white lines are ±1 standard deviation (Drinkwater et al., 1994 and Horne and Petrie, 1988)). 14
Figure 3. Standard deviation of SST anomalies (°C). 14
Figure 4. Standard deviation of SST anomalies (°C) for the four seasons. 15
Figure 5. Mean SST (°C). The colour map is enhanced for a more detailed resolution of SST on the Shelf. 16
Figure 6. Annual harmonic (°C) and phase (contours, d). 16
Figure 7. Semiannual harmonic amplitude (°C) and phase (contours, d). 17
Figure 8. Triannual harmonic amplitude (°C) and phase (contours, d). 17
Figure 9. Phase and amplitude of the annual (red), semiannual (green) and triannual (blue) harmonics. 18
Figure 10. The e-folding times (d) of weekly SST anomalies. 18
Figure 11. Effective number of independent observations from Nov. 1981 to Nov. 2000. 19
Figure 12. Spatial scales of variability of weekly sampled SST anomalies calculated as the distance (km) between each location and the 0.7 correlation coefficient averaged limit in all directions. 19

Figure 13. Mean distance (km) from each location to 0.7 correlation contour points. 20
Figure 14. Standard-deviation of distance (km) from each location to 0.7 correlation coefficient contour points. 20
Figure 15. Variation coefficient of distance from each location to 0.7 correlation coefficient contour points. 21
Figure 16. Correlation coefficients relative to pixels near AZMP fixed stations. 22
Figure 17. Correlation coefficients relative to Gulf of St. Lawrence and Scotian Shelf locations. 23
Figure 18. Correlation coefficients relative to pixels in Gulf of Maine and Grand Banks. 24
Figure 19. Spatial scales of weekly sampled and filtered (14 d to 91 d) SST anomalies. 25
Figure 20. Areas (grey) where AZMP fixed stations cover 50% and more of the SST anomaly variance. 26
Figure 21. Time series of SST anomalies for 3 by 3 pixel area centred on the AZMP fixed stations. 27
Figure 22. Spectra of SST anomalies for 3 by 3 pixel area centred on the AZMP fixed stations. 27
Figure 23. Time series of near-surface temperature at Cape Freels, Newfoundland. The grey line represents the original data, the thick black line the 2 week running mean filter , and the thin black line along the x axis, the difference between the original and filtered data (i.e., the series represented periods less than 2 weeks). 28
Figure 24. Time series of near-surface temperature at Banc Beaugé, Northeast Gulf of St. Lawrence. The grey line represents the original data, the thick black line the 2 week running mean filter , and the thin black line along the x axis, the difference between the original and filtered data (i.e., the series represented periods less than 2 weeks). 29

LIST OF TABLES

Table 1. Spatial scales associated with AZMP stations and other locations 10
Table 2. Distribution of Temperature Anomaly Variance for the AZMP fixed stations 10
Table 3. Temperature variance ($^{o}C^{2}$), Scotian Shelf-Gulf of Maine 11
Table 4. Temperature variance ($^{o}C^{2}$), Newfoundland Shelf 11
Table 5. Temperature variance ($^{o}C^{2}$), Gulf of St. Lawrence 12

ABSTRACT

Ouellet, M., B. Petrie and J. Chassé. 2003. Temporal and spatial scales of sea-surface temperature variability in Canadian Atlantic waters. Can. Tech. Rep. Hydrogr. Ocean Sci. No. 228: v + 30 p.

To determine how representative measurements of sea-surface temperature (SST) for the Atlantic Zonal Monitoring Program (AZMP) are, an analysis of the spatial and temporal variability of SST in Canadian Atlantic waters (40-52°N, 40-75°W) is presented. The basic dataset is weekly averaged SST from the Jet Propulsion Laboratory from 1981 to 2000 at a resolution of 18-km. Particular focus is given to the fixed stations of the AZMP that are located in the Anticosti Gyre, the Gaspé Current, the southwestern Gulf of St. Lawrence (Shediac Valley), off St. John's (Sta. 27), off Halifax (Sta. 2) and at the mouth of the Bay of Fundy (Prince 5). The mean, annual, semiannual and triannual harmonics and SST anomalies have been determined for 9253 pixels. The harmonics removed more than 85% of the variance of time series on the continental shelf, and more than 95% in some areas of the southern Gulf of St. Lawrence, Scotian Shelf and Gulf of Maine. In the region defined by the mean position ±1 standard deviation of the shelf-slope front, the harmonics accounted for 30% to 80% of the variance. Spatial scales were evaluated by computing mutual correlation coefficients between a series of SST anomalies at one location and the series for the rest of the grid. The average radial distance from the reference location to the 0.7 coefficient contour was defined as a measure of the length scale. The largest coherence scales, about 300 km, occur over the Grand Banks; anisotropy is important in areas located near the coast, large bathymetric variations or persistent oceanic features. The temporal variability was estimated as the e-folding scale of the temporal auto-correlation of the SST anomalies and ranges approximately from 1 to 3 weeks throughout the grid.

Ouellet, M., B. Petrie and J. Chassé. 2003. Temporal and spatial scales of sea-surface temperature variability in Canadian Atlantic w .ers. Can. Tech. Rep. Hydrogr. Ocean Sci. No. 228: v + 30 p.

RÉSUMÉ

Afin d'évaluer la représentativité des mesures de température de surface de la mer (TSM) pour le Programme de Monitorage de la Zone Atlantique (PMZA), une analyse de la variabilité spatiale et temporelle de la TSM dans les eaux canadiennes atlantiques (40-52°N, 40-75° W) est présentée. Les données utilisées consistent en la TSM moyenne par semaine, obtenue du Jet Propulsion Laboratory, de 1981 à 2000 à une résolution de 18 km. Une attention spéciale est prêtée aux stations fixes du PMZA, qui sont situées dans la gyre d'Anticosti, le courant de Gaspé, le sud-ouest du Golfe du Saint-Laurent (Vallée de Shédiac), au large de St. John's (Station 27), au large de Halifax (Station 2) et à l'embouchure de la Baie de Fundy (Prince 5). La moyenne, les harmoniques annuelle, semiannuelle et trianuelle, ainsi que les anomalies de TSM, furent déterminées pour 9253 pixels. Les harmoniques contribuent à plus de 85% de la variance des séries temporelles de TSM sur le plateau continental, et à plus de 95% dans certaines parties du Golfe du Saint-Laurent, du plateau néo-écossais et du Golfe du Maine. Dans la région définie par la position moyenne ±1 déviation standard du front plateau-pente, les harmoniques contribuent de 30% à 80% de la variance. Les échelles spatiales furent évaluées en calculant les coefficients de corrélation mutuels entre une série de TSM à un endroit et les séries du reste de la grille. La distance radiale moyenne entre le lieu de la série de TSM et son contour de coefficient de corrélation 0.7 est définie comme mesure d'échelle spatiale. Les plus grandes échelles de cohérence ainsi calculées, d'environ 300 km, se situent au-dessus des Grands Bancs. L'anisotropie des contours est importante dans les régions situées près de la côte, près d'importantes variations bathymétriques, ou encore de caractéristiques océaniques importantes. La variabilité temporelle fut estimée de l'autocorrélation temporelle des anomalies de la TSM selon le facteur d'échelle de repliement de e et s'étend approximativement de 1 à 3 semaines selon la position dans la grille.

1.Introduction

The Atlantic Zonal Monitoring Program is an operational marine research program conducted by DFO in the eastern Canadian waters (Northwestern Atlantic) since 1998 (Therriault et al., 1998). The coverage of physical, chemical and biological variables is limited by technical, financial and physical constraints. Consequently, in order to optimize the monitoring program, it is important to know the spatial and temporal scales of variability throughout the region. The station locations and dedicated monitoring cruises were decided based on limited data analyses, the most thorough of which focused on the Scotian Shelf (Therriault et al., 1998; Petrie and Dean-Moore, 1996).

In order to assess the ability of the AZMP fixed stations and transects to represent the oceanic variability on the Canadian Atlantic continental shelf and adjacent slope areas, a number of analyses have been undertaken using archived and ongoing datasets. In this report, we present the results of an investigation of the spatial and temporal scales of sea surface temperature (SST) variability in eastern Canadian waters using satellite infrared imagery data.

2.Data and Methods

2.1 Data

Satellite estimates of SST were extracted from the Ocean Sciences Database at the Bedford Institute of Oceanography (http://urchin.mar.dfo-mpo.gc.ca/sst/sst_main.html). This product was created by the Physical Oceanography Archive Centre of the Jet Propulsion Laboratory. The dataset was derived from the daytime NOAA Advance Very High Resolution Radiometer covering the period from November 1981 to November 2000 (data return was drastically reduced after November 2000 and the program terminated in February 2001). The time resolution is weekly and the spatial resolution is of approximately ~0.175° in both latitude and longitude, which in our region corresponds, on average, to 19.5 km along the north-south orientation and 13.6 km along the east-west orientation. Mason et al. (1998) concluded that the data were useful in examining long-term changes of SST in the region. The slope of the linear regression between frequently sampled oceanic stations and the satellite estimates was 1.04(±0.03) with an intercept of 0.08(±0.15)°C, an average difference of –0.37°C and a standard deviation of 1.27°C.

We extracted data in a region bounded by 40-52° N and 40-75° W (Fig. 1), obtaining series at 9253 different locations on a 68X194 grid.

2.2 Harmonic analysis and SST anomalies

Harmonic analysis was used to estimate the annual cycle of SST and the anomalies, defined as the difference between individual data points and the harmonic signal on the same day. For the purpose of the analysis, we define the annual cycle as the sum of the mean and the annual, semiannual (6 months) and triannual (4 months) harmonics. The amplitude and phase of each harmonic component at all locations were determined by least-square fitting. Expressing the SST as a time-dependent 2 dimensional field $\boldsymbol{T}$ ($\boldsymbol{x}$ and $\boldsymbol{y}$ being horizontal directions, and $\boldsymbol{t}$, time), the anomaly ($\boldsymbol{R}$) is defined as :

$$R(x,y,t) \equiv T(x,y,t) - A_0(x,y) - \sum_{k=1}^{3} A_k(x,y)\cos(k\omega t + \varphi_k(x,y))$$

where A_0 is the mean temperature, A_1, A_2, A_3 the annual, the semiannual and triannual harmonic amplitudes and φ_1, φ_2 and φ_3 the annual, semiannual and triannual harmonic phases. The fundamental frequency, ω, is the annual frequency ($2\pi/365$ d^{-1}). The contribution of the mean and the annual harmonic in our region to the annual cycle is readily understood. Our previous experience indicated that the semiannual harmonic offsets the annual harmonic in the winter when minimum SST values are reached and remain relatively constant for about 2 months. The triannual harmonic in some cases helps to account for the rapid temperature decrease in the late summer and early fall.

The quality of the harmonic fits depends on the distribution of data through the year. For instance, if only spring to fall observations are available, we found that the annual harmonic tended to be too large. The limitation of minimum winter water temperatures to about –1.85°C is an important constraint for this type of analysis since it transfers part of the signal from the annual frequency to the semiannual one. To avoid bias arising from low numbers of SST observation, limited by phenomenon such as cloud and ice cover, series without at least five (5) observations through the months of February and March and at least 50 observations overall were combined with series from locations within a radial range of 0.25°. If the resulting series from that combination did not satisfy the aforementioned criterion, the location was not included in the analysis. Otherwise, the harmonic analysis coefficients were determined from the composite series, but only the values from the original series of the location were used for the calculation of anomalies. The locations where such averaging was necessary, mostly because of ice cover, are shown in Fig. 1. They only account for 1.3 % of the pixels and are concentrated in the Strait of Belle Isle area. There are also a few sites in the Southern Gulf of St. Lawrence, the St. Lawrence Estuary and near Cape Cod.

2.3 Calculation of correlation coefficients

Zero time-lag correlations between time series at different pixels, i.e. the correlations are functions of the horizontal distance, and lagged temporal autocorrelations at each pixel were estimated from the anomalies. Halliwell et al. (1991) and Yashayaev and Logutov (1997) have used this method. With the notation expressed above, the matrix of correlation coefficients C can be expressed as a function of three variables:

$$C(p,\lambda,\tau) = \frac{\sum_{t=s}^{e-\tau}\left[\left(R(p,t)-\overline{R}(p)\right)\left(R(p+\lambda,t+\tau)-\overline{R}(p+\lambda)\right)\right]}{\sum_{t=s}^{e}\left(R(p,t)-\overline{R}(p)\right)\sum_{t=s}^{e}\left(R(p+\lambda,t+\tau)-\overline{R}(p+\lambda)\right)}$$

where $\overline{R}(p) = \sum_{t=s}^{e} R(p,t)$

and $p = p(x,y)$ is a co-ordinate related to spatial position, λ the distance to the position denoted by co-ordinate p, s and e are respectively the series start and end times, while τ is a time lag in same units as t.

At each pixel, correlations were calculated for the time series at various lags to determine the temporal autocorrelation function. The time lags were chosen from 0 to 364 days with increments of 7 days (data resolution). For pixels at different locations, the correlations were calculated for zero lag only, thus giving the spatial correlation function. In terms of the equation for $C(p,\lambda,\tau)$:

$$\lambda > 0 \rightarrow \tau = 0 \text{ spatial correlation}$$
$$\lambda = 0 \rightarrow \tau > 0 \text{ temporal correlation}$$

Since we have 9253 pixels, there were 9253*(9253/2-1) spatial correlation coefficients and 9253*51 temporal correlation coefficients to calculate.

It was necessary, because of data scarcity in some locations, to ensure that a minimum number of simultaneous observations were available before a correlation coefficient was calculated between series. After a number of trials, we set this number to 50. When this criterion was not met, one of the two series (generally the shortest one) was combined with series at its neighbouring locations (within a radius of 0.25°) in order to build larger series and attain at least 50 common times when there were data. If the criterion was met the correlation coefficient was calculated.

3.Results

3.1 Harmonic analysis

Over the continental shelf, the Gulf of Maine and Gulf of St. Lawrence, 85 to 99%, with an average of about 94%, of the SST variance is accounted for by the harmonic fits (Fig. 2). The amount of variance decreases over the continental slope at a location that generally corresponds to ±1 standard deviation from the mean position of the shelf-slope front south of Georges Bank, the Scotian Shelf and the Grand Banks. Off the eastern Grand Banks, the minimum in the percentage of the variance accounted for by the harmonic fit is roughly bounded by the ±1 standard deviation of the front from its mean position.

The standard deviations of the residuals were calculated for the entire series (Fig. 3). Over the continental slope and in the Gulf of St. Lawrence, the standard deviations are ~2°C. The maximum standard deviation of the residuals is bounded by the area described by 1± standard deviation of the shelf-slope front. The standard deviations of the residuals were also computed for different seasons and show the same general behaviour (Fig. 4). The variance over the shelves is lower in winter (standard deviations of ~1°C) because the water reaches its minimum temperature in the Gulf of St. Lawrence and on the Newfoundland Shelf.

The mean annual SST shows a number of well-known oceanographic features (Fig. 5). The colder waters flowing from the Labrador Shelf are visible as two distinct flows, the inshore branch of the Labrador Current through Avalon Channel and the offshore branch roughly along the 200 m isobath on the eastern edge of Grand Bank. The surface manifestation of offshore

branch of the Labrador Current disappears at the Tail of Grand Bank. The southwestern Grand Bank shows the influence of onshore movement of warmer, upper slope waters. The inshore branch of the Labrador Current is seen rounding the southern Avalon Peninsula and tending to move west toward Haddock and Halibut Channels.

In the Gulf of St. Lawrence, the coldest annual mean temperatures are found along the north shore; this is probably caused by the inflow of colder Labrador Shelf water through Belle Isle Strait and the tendency for persistent wind-driven upwelling, both processes augmenting the annual cycle of heat exchange with the atmosphere. The other area of low annual temperatures is the St. Lawrence Estuary, a region known for strong vertical mixing and upwelling. The area adjacent to Prince Edward Island has the highest annual temperatures in the Gulf.

There is a distinct impression of the influence of the colder annual temperatures that are advected from the Gulf through Cabot Strait onto the Scotian Shelf. It can been seen as an inshore branch south of Cape Breton, the Nova Scotia Current, and on the western edge of the Laurentian Channel moving along the shelf break towards Sable Island. The penetration of warm upper slope waters onto the central Scotian Shelf over Emerald and Western Banks is visible. The surface expression of the Nova Scotia Current remains confined to the coast before spreading offshore to the west of Halifax. The colder upwelling zone off southwest Nova Scotia is clearly seen, as well as the cooler area of the mouth of the Bay of Fundy and the gradient of temperature along the Bay. Georges Bank and the Gulf of Maine annual temperatures are in the same range, about 10-12°C, as those over the upper slope. The +1 standard deviation line north of the shelf-slope front from Georges Bank to north of Flemish Cap corresponds roughly to the 11°C mean annual temperature isoline.

The amplitudes of the annual harmonic are generally larger over the continental shelf and in the Gulf of St. Lawrence than in the deep water areas (Fig. 6). The largest amplitudes, approximately 10.6 °C, are found in the southern Gulf of St. Lawrence where, in some areas, shallow depths confine the heat input leading to large annual harmonics; in deeper areas, the large freshwater inflows in the Gulf allow for the development of a strongly-stratified, shallow surface layer also leading to elevated annual harmonic amplitudes. Moreover in winter, water temperatures are near the freezing point for salt water. Thus the annual SST range is very high. In contrast, the St. Lawrence Estuary has a small annual harmonic (~4°C) because strong vertical mixing and upwelling of deeper cool waters limits the summer SST. The influence of the Gulf outflow is seen on the Scotian Shelf as a band of coastal water with a large annual harmonic. This region stretches from the Sydney Bight to the west of Halifax where veers offshore. Again this is the influence of the Nova Scotia Current that was apparent, but less compelling, in the mean annual temperature field. As in the St. Lawrence Estuary, the areas off southwestern Nova Scotia, the Bay of Fundy and the coastal region of Maine feature low amplitudes of the annual harmonic. This is caused by tidally induced mixing that spreads the atmospheric heat fluxes over a thicker upper layer and thereby reduces the harmonic amplitude. A similar situation is apparent over Georges Bank except for the central region where shallow depths limit the thickness of the upper layer and results in a higher annual harmonic amplitude. The amplitude of the annual harmonic decreases significantly at the shelf-slope front from Georges Bank to the Tail of Grand Bank. The advective influence of cold water can be seen in the Newfoundland region, particularly on the Northeast Newfoundland Shelf. The area directly south of the Tail and along the southwest

slope of Grand Bank has large harmonic amplitude that may be caused by on-bank movement of warmer slope water in the summer and off-bank movement of colder shelf waters in winter.

The phases of the annual harmonic change by only about 20 d over the shelf, Gulf of St. Lawrence and Gulf of Maine regions. Peak temperatures associated with the annual harmonic are found from about day 220 (Aug. 8) to 240 (Aug. 28). This is expected because the solar heating cycle is highly coherent over the region.

The semiannual harmonic amplitudes have a maximum value of 2.2°C (Fig. 7). Large regions with amplitudes of about 2°C are found in the Gulf of St. Lawrence and over the eastern Newfoundland Shelf. These areas have winter surface temperatures that are close to the freezing point of salt water and remain nearly constant for periods of about 2 months.

The mean and annual harmonic together tend to give temperatures that are too low during winter; the semiannual harmonic, with its peak amplitudes from day 30-50 (Feb-Mar) is out of phase with the annual and counteracts its tendency to give SST values well below the freezing point. It is noticeable that the semiannual harmonic is low in areas of strong mixing such as southwest Nova Scotia, the Bay of Fundy, the Maine coastal region and Georges Bank. Two areas have unexpectedly high semiannual harmonic amplitudes – the western Gulf of Maine and the area off the Tail of Grand Bank.

The triannual harmonic amplitudes (Fig. 8) are patchy, particularly in the deep water region, and have a range of 0.0 to 1.5°C over the entire region. The highest values are found in the vicinity of the shelf-slope front, south and northwest Gulf of St. Lawrence, and in the Esquiman Channel. The variation of the phases is large (Fig. 8, 9); however, over the continental shelves and in the Gulf of St. Lawrence, the amplitude patterns and the range of phases (75-100) are quite consistent.

A scatter-plot of annual, semiannual and triannual harmonic amplitudes vs. phase (Fig. 9) shows that the phases of annual harmonic are narrowly confined between August and early September. The semiannual harmonic is centred around mid-August which means that it also has a peak in February opposing the minimum of the annual harmonic. We show the August peak of the semiannual harmonic to improve the overall figure presentation. The phase of the triannual harmonic is largely confined to July and August (as with the semiannual harmonic, the triannual has multiple peaks; July-August maxima also means there are peaks in March-April and November December), but there are a number of values in May and June.

3.2 Temporal scales of variability

The e-folding time (d) of the temporal autocorrelation function was determined from an exponential fit of weekly SST anomalies at all pixels as an index of temporal persistence (Fig. 10). The centre of Georges Bank and southwestern Grand Banks are areas with highest temporal persistence of 2-3 weeks. Over most of the grid, correlation coefficients fall to 0.37 within 1 to 2 weeks. Monthly and seasonal anomalies were also examined with similar results. The number of observations decreases dramatically north of 50° N and east of 50° W and is largely because of data storage limitations when the archive was initiated. The confidence limits or statistical uncertainty for a particular quantity such as the mean depends on the number of degrees of

freedom, often taken as the number of observations. However, time series of ocean properties tend to be autocorrelated and thus have fewer degrees of freedom. The autocorrelation coefficients (c_i) were used to determine the effective number of independent observations (n^*), following the expression given by Bayley and Hammersley (1946):

$$\frac{1}{n^*} = \frac{1}{n} + \frac{2}{n^2}\sum_{i=1}^{m}(m+1-i)c_i$$

where n is the total number of observations in the series, m is the number of samples after which the temporal autocorrelation reaches zero or, more practically, a noise level. We have set this value to e-folding scale times 1.5.

The effective number of independent observations for the 19 covered years are mapped on Fig. 11, and are important in the interpretation of several results presented in this study. The data reduction north of 50° N and east off 50° W is apparent. Some other areas showing few observations can be explained by ice cover or clouds limiting data return (Mason et al., 1998). The areas with higher persistence have fewer independent observations than locations with lower persistence.

3.3 Spatial coherence scales of variability

Spatial scales of variability at each pixel were estimated using two different methods. The first method consists of ordering correlation coefficients by distance alone from the central pixel and then fitting (least-square) a linear function to them. The method is illustrated using a single pixel (Appendix I). The 0.7 correlation coefficient intercept is then taken as the spatial scale of variability for each pixel (Fig. 12) and is independent of direction.

This largest spatial scales (~200-300 km) are found over the Grand Banks. Intermediate scales of ~100-175 km occur over the Northeast Newfoundland Shelf, Flemish Cap, much of the Gulf of St. Lawrence and the Scotian Shelf. The smallest horizontal scales are found seaward of the shelf break, in the Gulf of Maine, the St. Lawrence Estuary and the Gaspé Current.

A second method was designed to allow for the determination of the isotropy (or anisotropy) of the scales of variability. It consists of interpolating the 0.7 values as a contour around a central pixel, then computing the mean and standard deviation of distance between every contour point and the origin. The mean is an indication of the magnitude of the scale (Fig. 13), like the scale computed in the method previously described. The standard-deviation (Fig. 14) is an indication of the absolute anisotropy of the contours, and when normalized by dividing the mean (variation coefficient, Fig. 15), it is an indication of the relative anisotropy (a value of 0 indicating a perfectly circular contour, the higher the value, the greater the anisotropy).

The distribution of the magnitude of the spatial scales derived by both methods is essentially the same. The variation coefficients show that the most isotropic contours occur over the Grand Banks, perhaps related to the strong advection of contrasting temperature fields through the region and seen in the mean SST and the harmonics (Fig. 5-7).

The distributions of correlation coefficients relative to the AZMP stations, and to other selected locations in other regions (Fig. 16 to 18 and Table I) show that the largest area (scale of ~190 km) is captured by the observations from Sta. 27 off St. John's, Newfoundland. The correlation field associated with Station 2 on the Scotian Shelf, off Halifax, also represents a large area (scale of ~135 km) and reflects to a large extent the mean pathway of the Nova Scotia Current as depicted by models. The correlation field at the Shediac Valley fixed station is highly isotropic (variation coefficient of 0.1) and appears to account for the temperature anomalies over the western half of the Magdalen Shallows (scale of ~95 km). A similar scale is found for Anticosti Gyre station, but the variation coefficient shows that it is less isotropic (0.4) than Shediac. The correlation fields fall off sharply at short distance for the Gaspé and Prince 5 sites (scales of ~65 and ~50 km), with variation coefficients of 0.2 and 0.3. East Point, Esquiman and Belle Isle were proposed as monitoring stations but were never sampled. Our analysis shows that they would allow for coverage of large areas (~150, ~115 and ~204 km) in locations otherwise not currently sampled as AZMP fixed stations. Locations near important bathymetric variations (Rimouski, Strait of Belle Isle, Cabot Strait, Southeast Shoal, Flemish Pass) have large variation coefficients, which are indicative of non-circular coefficient contours.

3.4 Spatial coherence scales of variability at different sampling frequencies

In order to determine the dependence of the spatial scales of the SST anomalies on the sampling frequency, we recalculated them using filtered data at different frequencies. In each case, a low-pass boxcar filter was used. Spatial scales for the different cases considered (Fig. 19) show that on average, but especially on the Grand Banks, Scotian Shelf and Gulf of St. Lawrence, the scales of variability are smaller when the series are filtered at 14 and 30 d periods compared to the series at original sampling (7 days). However, filtering to 91 d (a lower frequency) results in slightly larger scales.

4. Conclusion

Spatial scales at selected locations and co-ordinates are summarised in Table 1. The coverage (accounting for at least 50% of the SST anomaly variance) of the actual AZMP configuration (Fig. 20) indicates that the fixed stations alone could not adequately describe the variability of the SST anomalies for most of the region. Moreover, the temporal scales of variability indicate that weekly sampling is required. It remains to be determined if the same is true for temperature at other depths and for other variables (including chemical and biological variables) throughout the shelf region. Remote sensing is essential to account for the SST variability.

There are two important limitations of the SST time series. The first limitation is the potential for gaps in the series because of clouds obscuring the sea surface and because of ice cover, a significant factor in the Atlantic region. The second limitation is that the sampling frequency of 1 week limits the temporal resolution of the variance. If significant variability occur at periods shorter than 2 weeks (the shortest period resolved by a series sampled weekly), then the SST time series could be aliased.

We addressed the first limitation by creating temperature anomaly time series for a 3 by 3 pixel area centred on each of the AZMP fixed stations (Fig. 21). For the Gaspé, Shediac, Stn. 2, Prince 5 and Stn. 27 sites, the interval between successive samples was 1 week (i.e., no data gap)

for 76, 80, 79, 65, 63% of the time. When gaps did occur they tended to be large since the overall percentage data return from October 1981 to October 2000 was 48, 54, 64, 50 and 46% respectively. The highest data return is for Stn. 2, a site not affected by ice. We computed the spectra for each of the anomaly time series (the mean and first 3 harmonics removed, Fig. 22). The data series then were divided into blocks of 260 weeks (5 years), the mean for each block removed and missing data set equal to 0. This latter procedure removes some of the low frequency variance. The integrals of the variance for these spectra are 1.55, 1.23, 1.17, 0.58 and 0.96 $^{o}C^{2}$ for Gaspé, Shediac, Stn. 2, Prince 5 and Stn. 27. All are lower than the variance in the anomaly series by 2 to 11%, which is expected because we removed block averaged temperature anomalies. The partition of variance in frequency bands is given in Table 2. At all sites the 2 highest frequency bands have the greatest percentage of variance. This makes it more compelling to examine the variance for periods shorter than 2 weeks.

To accomplish this we obtained a listing of all temperature recorders that were moored in depths of less than 5 m on the Newfoundland Shelf, the Gulf of St. Lawrence and the Scotian Shelf-Gulf of Maine region. Nearly all of these time series were located at the coast. A very limited number of records came from the offshore but these were generally of short duration and/or from unreliable instruments. From this list we extracted the raw records for sites that we judged to be most representative of the open shelf region. For each record we filtered the data with a 2 week running mean boxcar filter, subtracted the resulting time series from the original data thus obtaining a high-passed dataset; then we evaluated the seasonal variance for periods longer and shorter than 2 weeks. Sample series from the Newfoundland Shelf and the Gulf of St. Lawrence are shown in Fig. 23 and 24. The results are shown in Tables 3 to 5. The analysis indicates that the high frequency temperature variability can be as large as ~2^{o}C (standard deviation), with an average of about 0.9^{o}C and accounting for about 40 % of the variance in the records. We conclude that the temperature variance at periods shorter than 2 weeks is therefore a significant portion of the overall variance. It must be considered either directly (though sampling more frequently than 1 week) or indirectly (by estimating the potential statistical uncertainties) when examining interannual variability from in situ fixed station records or from the satellite SST observations.

5. Acknowledgements

The work underlying this report was funded by the Science Strategic Fund. We would like to thank Doug Gregory (Ocean Sciences Division, Bedford Institute of Oceanography) for providing us the JPL SST data. We thank Brenda Topliss, César Fuentes-Yaco, Denis Lefaivre and Pierre Larouche whose reviews led to clarifications and improvements in the report. Finally, we thank Bernard Pettigrew (IML) and Joe Craig (NWAFC) who provided the shallow water time series from the Gulf of St. Lawrence and the Newfoundland Shelf that allowed us to examine the high frequency variance in temperature time series.

6. References

Bayley and Hammersley, 1946. The effective number of independent observations in an autocorrelated series. J R. Statist. Soc. B8 : 184-197.

Drinkwater K.F., R.A. Myers, R. G. Pettipas and T.L. Wright, 1994. Climatic data for the northwest Atlantic: the position of the shelf/slope front and the northern boundary of the Gulf Stream between 50oW and 75oW, 1973-1992. Can. Data Rep. Fish. Ocean Sci. 125, iv + 103 pp.

Halliwell, G.R., P. Cornillon and D.A. Byrne, 1991. Westward-Propagating SST anomaly Features in the Sargasso Sea, 1982-1988. J. Phys. Oceanogr. 21 : 635-649.

Horne, E. and B. Petrie, 1988. Mean Position and Variability of the Sea Surface Temperature Front East of the Grand Banks. Atmos.-Ocean. 26 (3) : 321-328.

Mason, C.S., B. Petrie and B.J. Topliss, 1998. Satellite measurement of Sea-Surface Temperatures and the Study of Ocean Climate. Can. Tech. Rep. Hydrogr. Ocean Sci. 193, vii + 101 pp.

Petrie and Dean-Moore, 1996. Temporal and spatial scales of temperature and salinity on the Scotian Shelf. Can. Tech. Rep. Hydrogr. Ocean Sci. 177: viii + 45 pp.

Petrie, B. and C.S. Mason, 2000. Satellite Measurements of Sea Surface Temperature: an Application to Regional Ocean Climate. CSAS Res. Doc. 00/61, 25 pp.

Therriault, J.-C., B. Petrie, P. Pepin, J. Gagnon, D. Gregory, J. Helbig, A. Herman, D. Lefaivre, M. Mitchell, B. Pelchat, J. Runge, and D. Sameoto, 1998. Proposal for a northwest Atlantic zonal monitoring program. Can. Tech. Rep. Hydrogr. Ocean Sci. 194: vii + 57 pp.

Yashayaev, I. and O.G. Logutov, 1997. Spatial-Temporal Scales and Dynamics of the Sea Surface Temperature Anomalies in the North Atlantic. Oceanology (Translated from Okeanologiya). 38 (2) : 158-169.

Table 1. Spatial scales associated to AZMP stations and other locations

Reference names (bold types indicate AZMP stations)	Latitude °N	Longitude °W	Distance between pixel centre and station (km)	Dist. (km)	Mean (km)	SD (km)	Var. Coef.
Rimouski	48.779	-68.115	*N/a*	60	49	19	0.4
Anticosti Gyre	**49.658**	**-66.182**	***8***	**100**	**88**	**38**	**0.4**
Gaspé Current	**49.307**	**-66.182**	***8***	**65**	**61**	**13**	**0.2**
Shediac	**47.725**	**-64.072**	*7*	**95**	**90**	**13**	**0.1**
East Point	46.67	-61.787	*N/a*	150	151	26	0.2
Esquiman	48.955	-60.029	*N/a*	115	122	30	0.2
Belle Isle	50.01	-57.92	*N/a*	205	204	84	0.4
Cabot Strait	47.373	-59.854	*N/a*	130	124	33	0.3
West Scotian Shelf	43.154	-64.951	*N/a*	75	72	14	0.2
Station 2	**44.209**	**-63.193**	*7*	**135**	**137**	**26**	**0.2**
East Scotian Shelf	45.088	-57.041	*N/a*	170	174	33	0.2
Georges Bank	41.221	-67.588	*N/a*	50	46	12	0.3
Gulf of Maine	42.803	-67.939	*N/a*	90	89	18	0.2
Prince 5	**44.912**	**-66.709**	***11***	**55**	**48**	**15**	**0.3**
St-Pierre	45.967	-55.986	*N/a*	195	198	41	0.2
South East Shoal	44.033	-50.01	*N/a*	120	104	30	0.3
Hibernia	47.022	-48.955	*N/a*	180	185	51	0.3
Flemish Pass	47.022	-47.373	*N/a*	90	85	33	0.4
Station 27	**47.549**	**-52.471**	***9***	**190**	**195**	**41**	**0.2**
North Shoulder	48.955	-50.01	*N/a*	125	124	37	0.3
Northeast Newfoundland Shelf	50.889	-53.174	*N/a*	75	77	14	0.2

Table 2. Distribution of Temperature Anomaly Variance for the AZMP fixed stations

VARIANCE	Gaspé		Shediac		Stn.2		Prince 5		Stn. 27	
Band (period)	($°C^2$)	%	($°C^2$)	%	($°C^2$)	%	($°C^2$)	%	($°C^2$)	%
2-4 weeks	0.44	29	0.30	24	0.32	27	0.20	34	0.29	30
1-3 months	0.56	36	0.32	26	0.30	26	0.17	29	0.23	24
3-6 months	0.28	18	0.20	16	0.20	17	0.05	9	0.10	10
6 months-1 year	0.16	11	0.26	21	0.11	10	0.05	9	0.14	15
1 - 5 years	0.09	6	0.15	12	0.24	21	0.11	18	0.19	20
Total	1.55	100	1.23	100	1.17	100	0.58	100	0.96	100

Table 3. Temperature variance, Scotian Shelf-Gulf of Maine

Area	Depth (m)	Period	T>2 weeks (°C)²	T<2 weeks (°C)²	Ratio% high/low	SD high (°C)
CSS		AMJ	2.72	1.34	49	1.16
Off St. Margaret's Bay		JAS	3.74	2.36	63	1.54
		OND	0.52	0.66	128	0.81
		JFM	1.16	0.11	10	0.34
		AMJ	2.67	0.73	27	0.85
		JFM	0.29	0.11	37	0.33
SWNS		JAS	3.08	0.40	13	0.63
Fundy		JFM	2.02	0.08	04	0.29
Off St. Andrew's N. B.		AMJ	1.06	0.45	42	0.67
		AMJ	0.94	0.31	33	0.56
		AMJ	1.12	0.61	54	0.78
		OND	3.43	0.09	03	0.30
		JAS	1.03	0.37	36	0.61
		JAS	1.20	0.29	24	0.54

Table 4. Temperature variance, Newfoundland Shelf

Area	Depth (m)	Period	T>2weeks (°C)²	T<2weeks (°C)²	Ratio % high/low	SD high (°C)
Cape Freels		JAS	5.43	3.93	72	1.98
		JAS	1.00	1.52	152	1.23
		OND	4.72	0.45	09	0.67
		AMJ	2.12	1.56	74	1.25
		JAS	3.81	2.62	69	1.62
		OND	6.26	0.17	03	0.41
		AMJ	8.88	1.91	21	1.38
		JAS	3.82	1.49	39	1.22
Melrose		JAS	3.62	2.68	74	1.64

Table 5. Temperature variance, Gulf of St. Lawrence

Area	Depth (m)	Period	T>2weeks (°C)²	T<2weeks (°C)²	Ratio (%) high/low	SD high (°C)
Banc Beaugé (NorthEast Gulf of St. Lawrence) LON -60.07° LAT 49.51°	1	AMJ 1998	2.04	0.33	16	0.58
		1999	3.46	0.43	13	0.66
		2000	4.67	0.49	10	0.70
		2001	5.68	0.34	6	0.58
		JAS 1998	3.22	0.61	19	0.78
		1999	0.84	0.43	52	0.66
		2000	4.29	0.60	14	0.77
		2001	1.34	0.62	46	0.79
		OND 1998	0.85	0.30	36	0.55
		1999	6.90	0.87	13	0.93
		2000	1.19	0.45	38	0.67
		2001	1.80	0.14	8	0.37
Irving Whale (Southern Gulf of St. Lawrence) LON –63.39° LAT 47.40°	0.5	AMJ 1999	5.75	0.67	12	0.82
		2000	2.85	1.25	44	1.12
		2001	17.39	0.62	4	0.79
		JAS 1999	2.69	0.94	35	0.97
		2000	4.71	0.43	9	0.66
		2001	3.05	0.47	16	0.69
		OND 1999	5.66	0.12	2	0.35
		2000	1.49	0.32	22	0.57
		2001	8.63	0.53	6	0.72
Mont-Louis (Western Gulf of St. Lawrence) LON –65.73° LAT 49.53°	0.35	AMJ 1999	5.70	2.97	52	1.72
		2000	4.87	1.34	28	1.16
		2001	2.92	1.45	50	1.20
		JAS 1999	2.22	1.06	48	1.03
		2000	7.07	2.52	36	1.59
		2001	3.36	1.03	31	1.02
		OND 1999	5.33	0.54	10	0.73
		2000	0.81	0.15	18	0.39
		2001	1.02	1.26	124	1.12

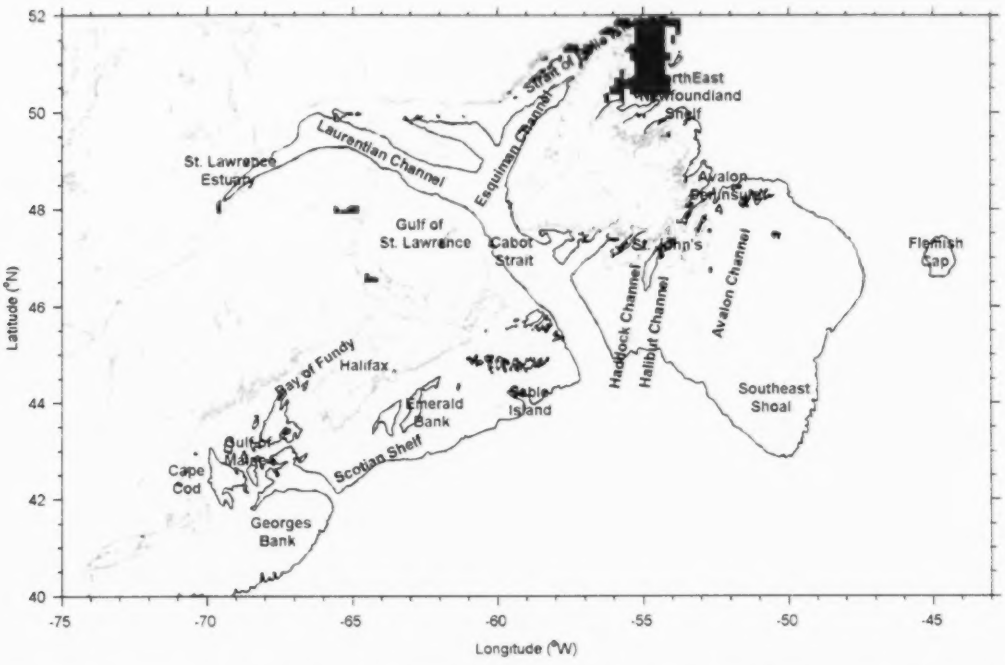

Figure 1. Names and locations of places mentioned in the text and locations (red pixels) where neighbour averaging was necessary to extract the harmonic signal.

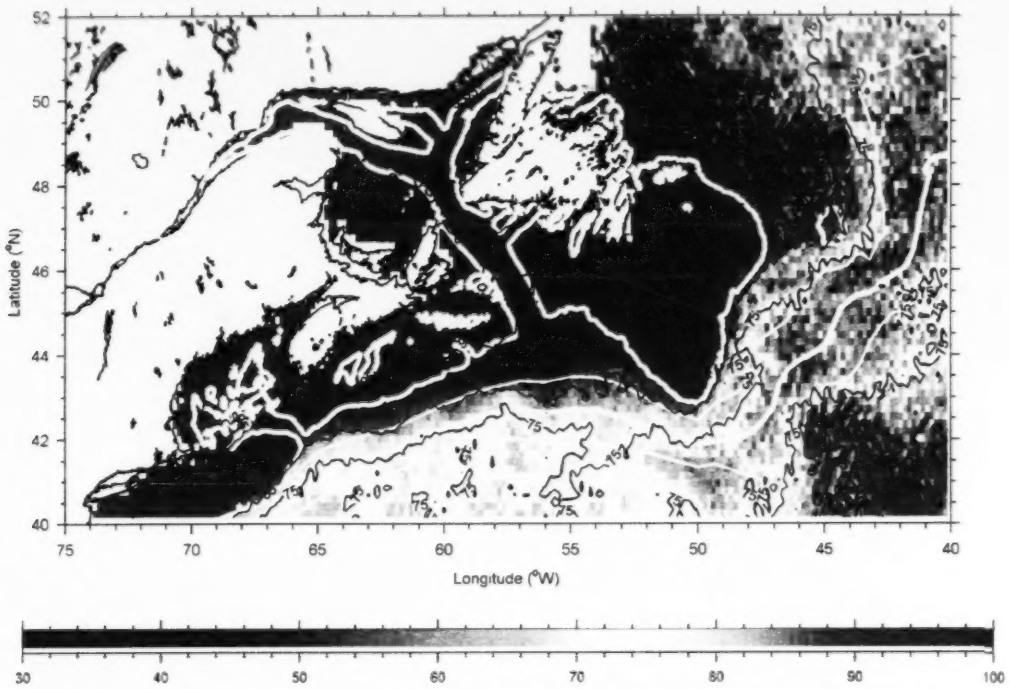

Figure 2. Percentage of total variance of the SST accounted for by the harmonic fit (the dotted line is the 200 m isobath, the thick white line is the shelf-slope front mean position and the thin white lines are ±1 standard deviation (Drinkwater et al., 1994 and Horne and Petrie, 1988)).

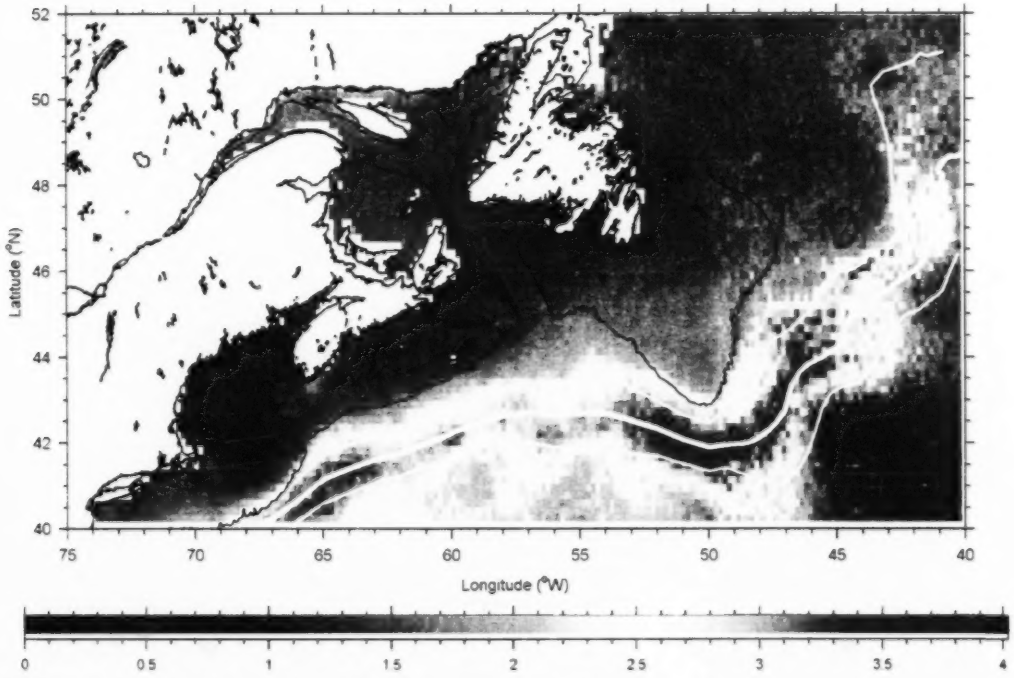

Figure 3. Standard deviation of SST anomalies (°C).

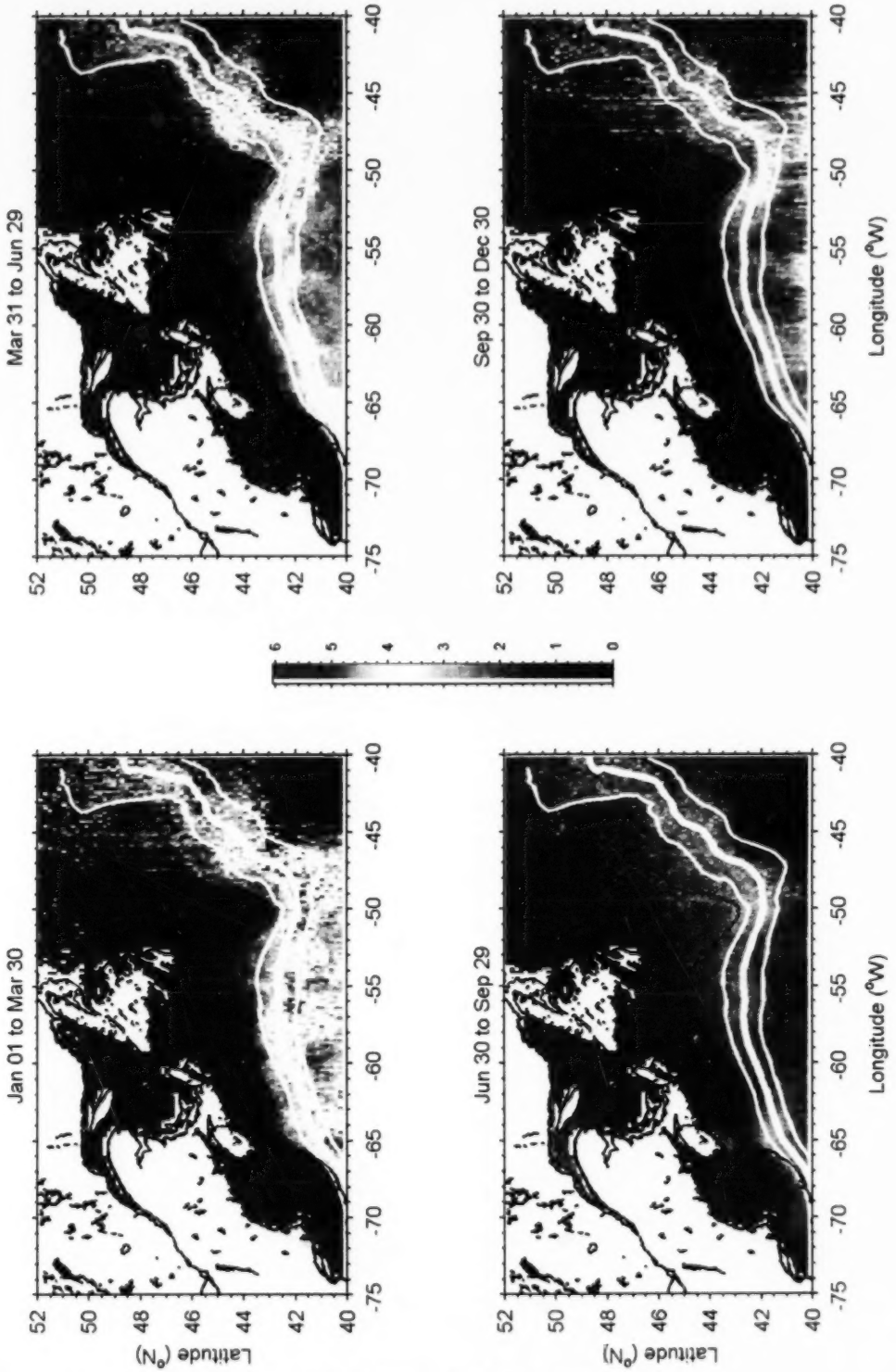

Figure 4. Standard deviation of SST anomalies (°C) for the four seasons.

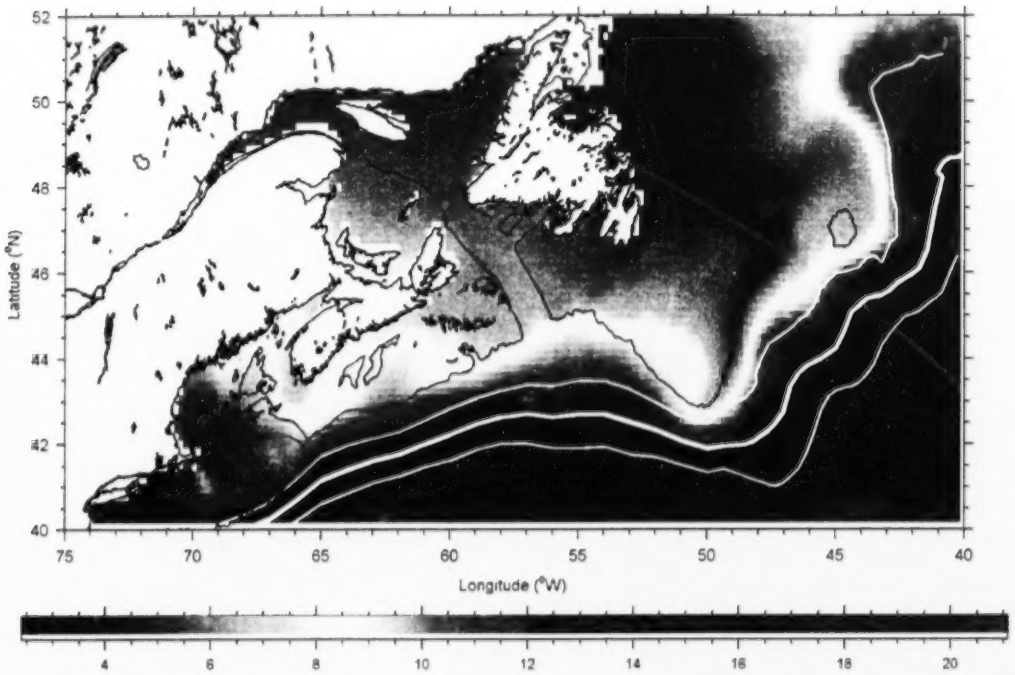

Figure 5. Mean SST (°C). The colour map is enhanced for a more detailed resolution of SST on the Shelf.

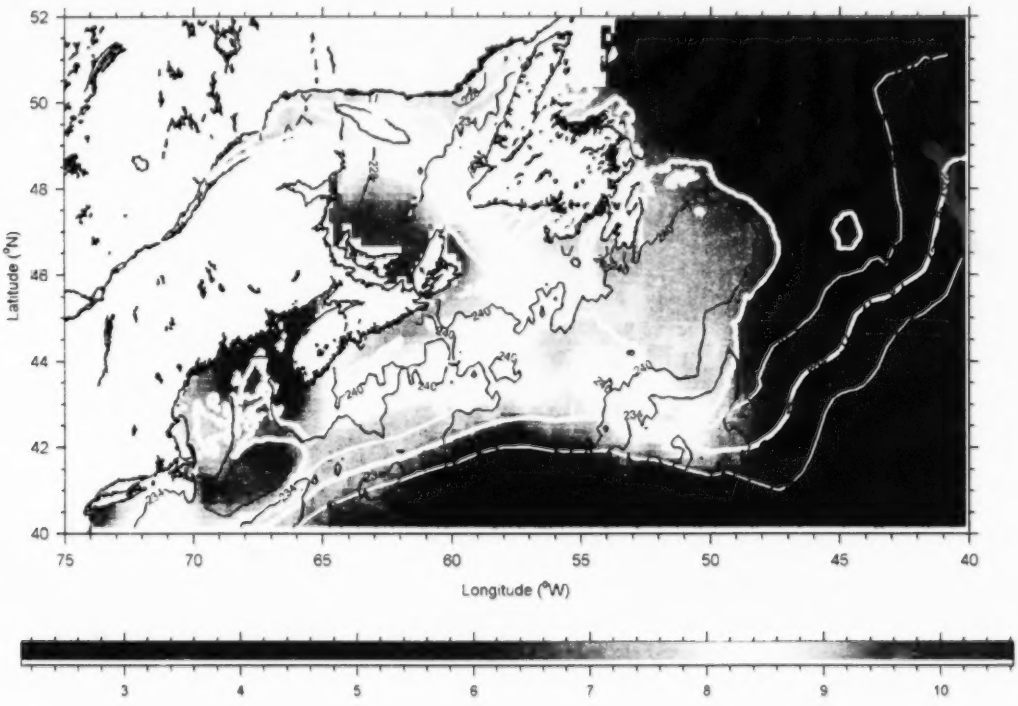

Figure 6. Annual harmonic (°C) and phase (contours, d).

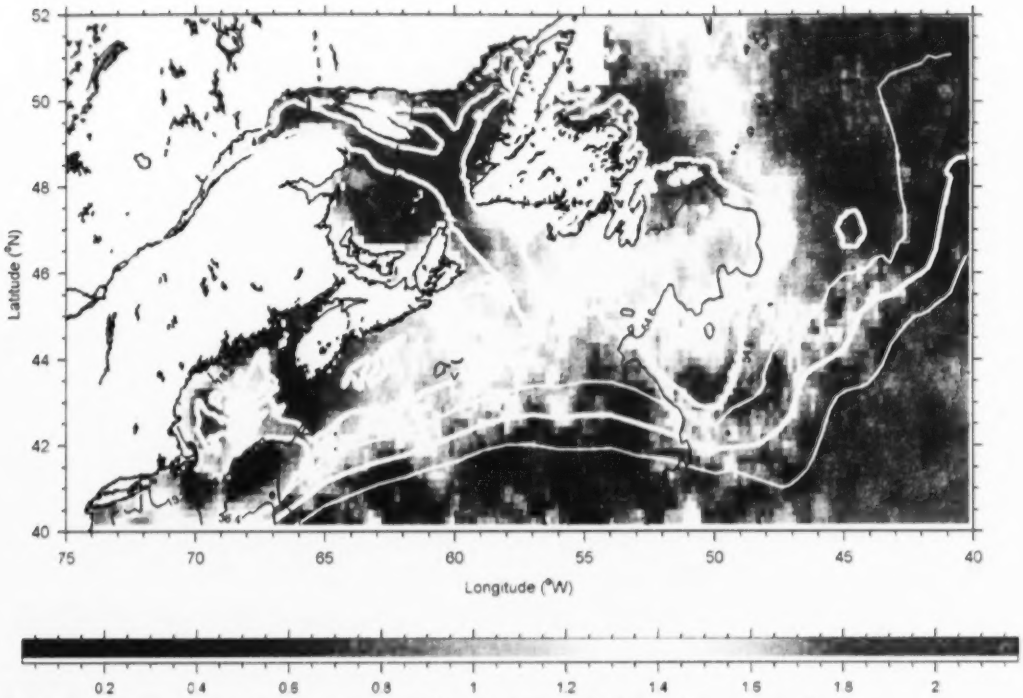

Figure 7. Semiannual harmonic amplitude (°C) and phase (contours, d).

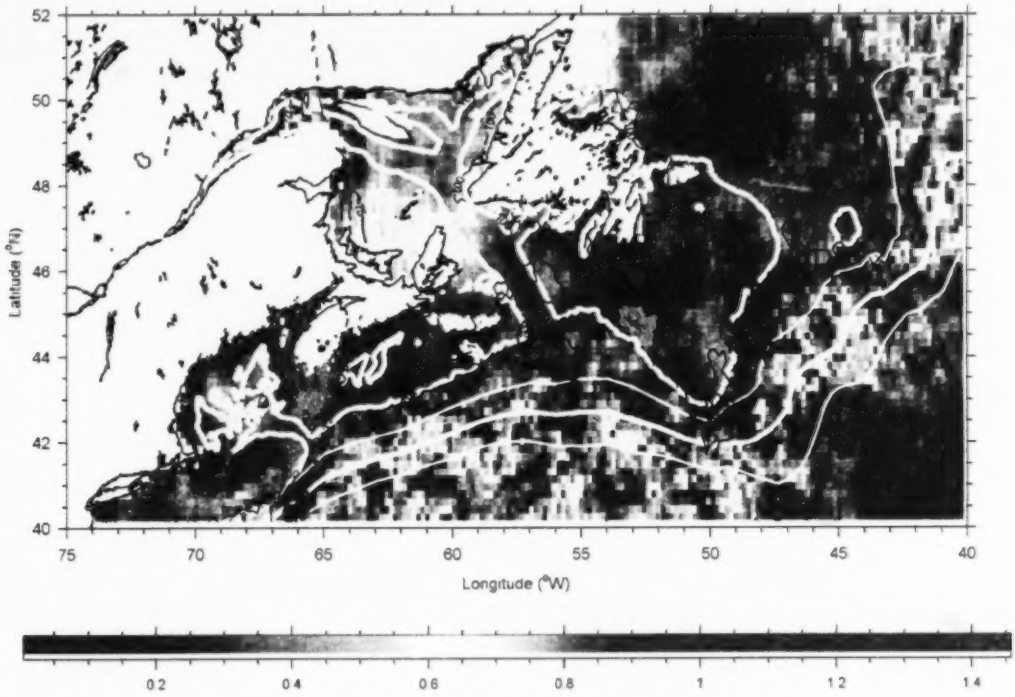

Figure 8. Triannual harmonic amplitude (°C) and phase (contours, d).

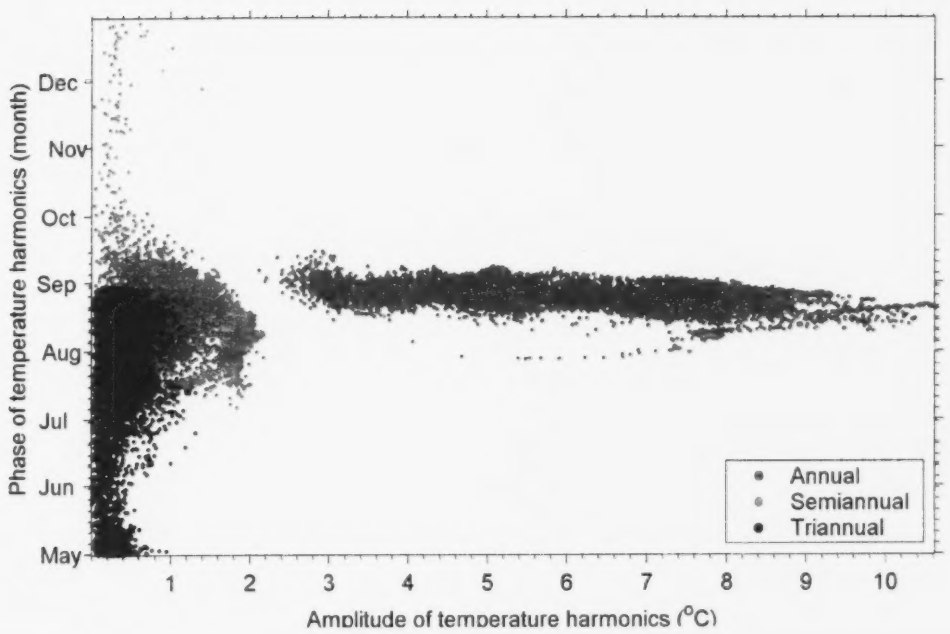

Figure 9. Phase and amplitude of the annual (red), semiannual (green) and triannual (blue) harmonics.

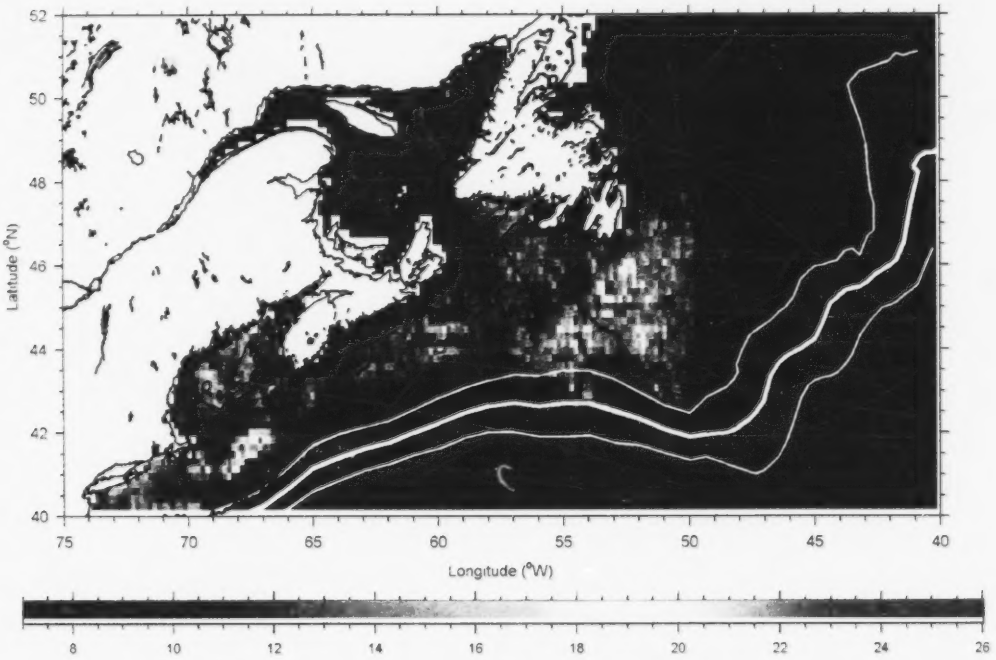

Figure 10. The e-folding times (days) of weekly SST anomalies.

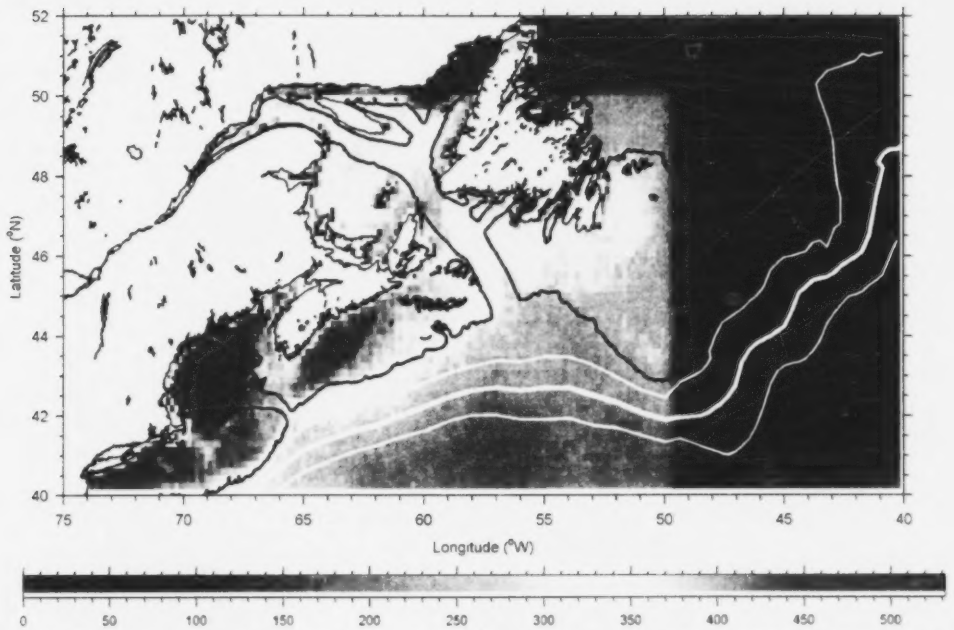

Figure 11. Effective number of independent observations from Nov 1981 to Nov 2000.

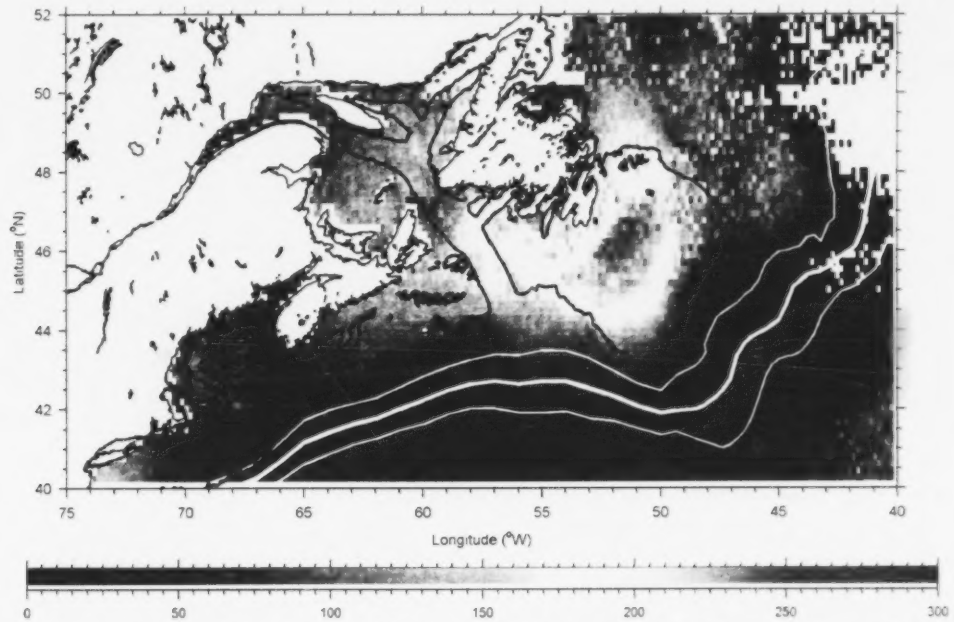

Figure 12. Spatial scales of variability of weekly sampled SST anomalies calculated as the distance (km) between each location and the 0.7 correlation coefficient averaged limit in all directions.

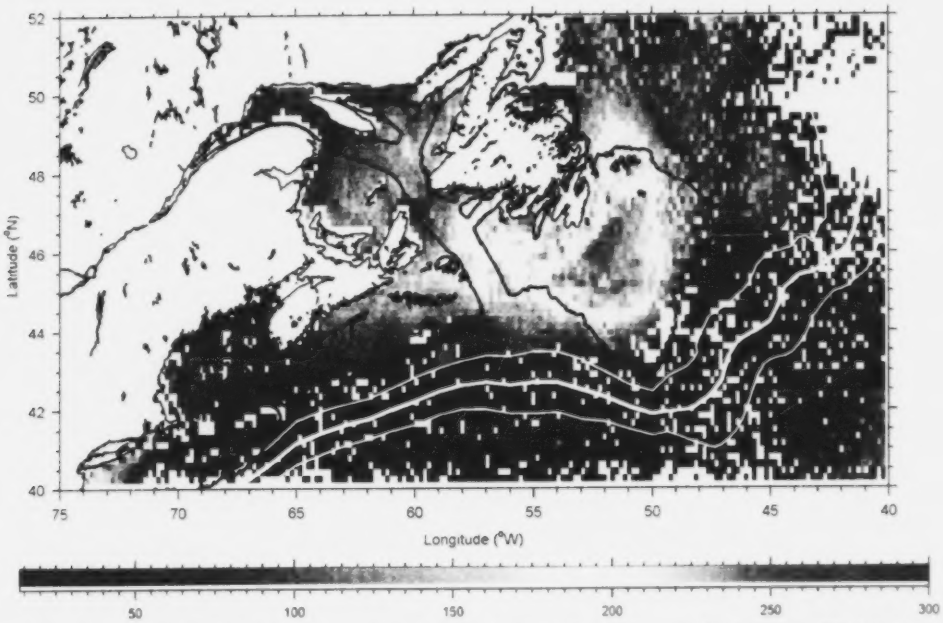

Figure 13. Mean distance (km) from each location to its 0.7 correlation coefficient contour points.

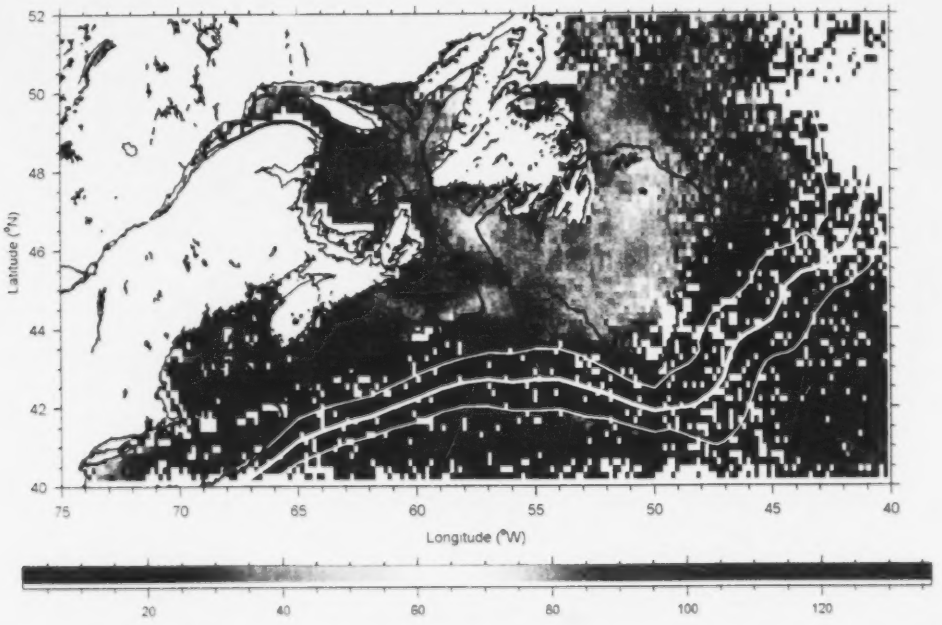

Figure 14. Standard-deviation of distance (km) from each location to its 0.7 correlation coefficient contour points.

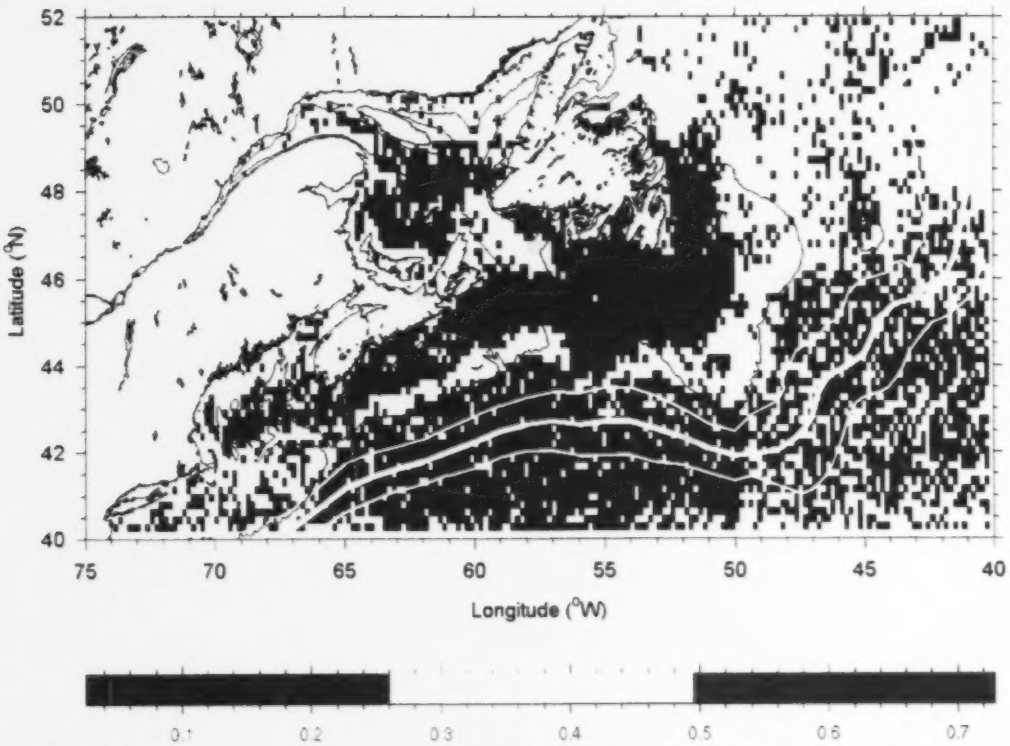

Figure 15. Variation coefficient of distance from each location to its 0.7 correlation coefficient contour points.

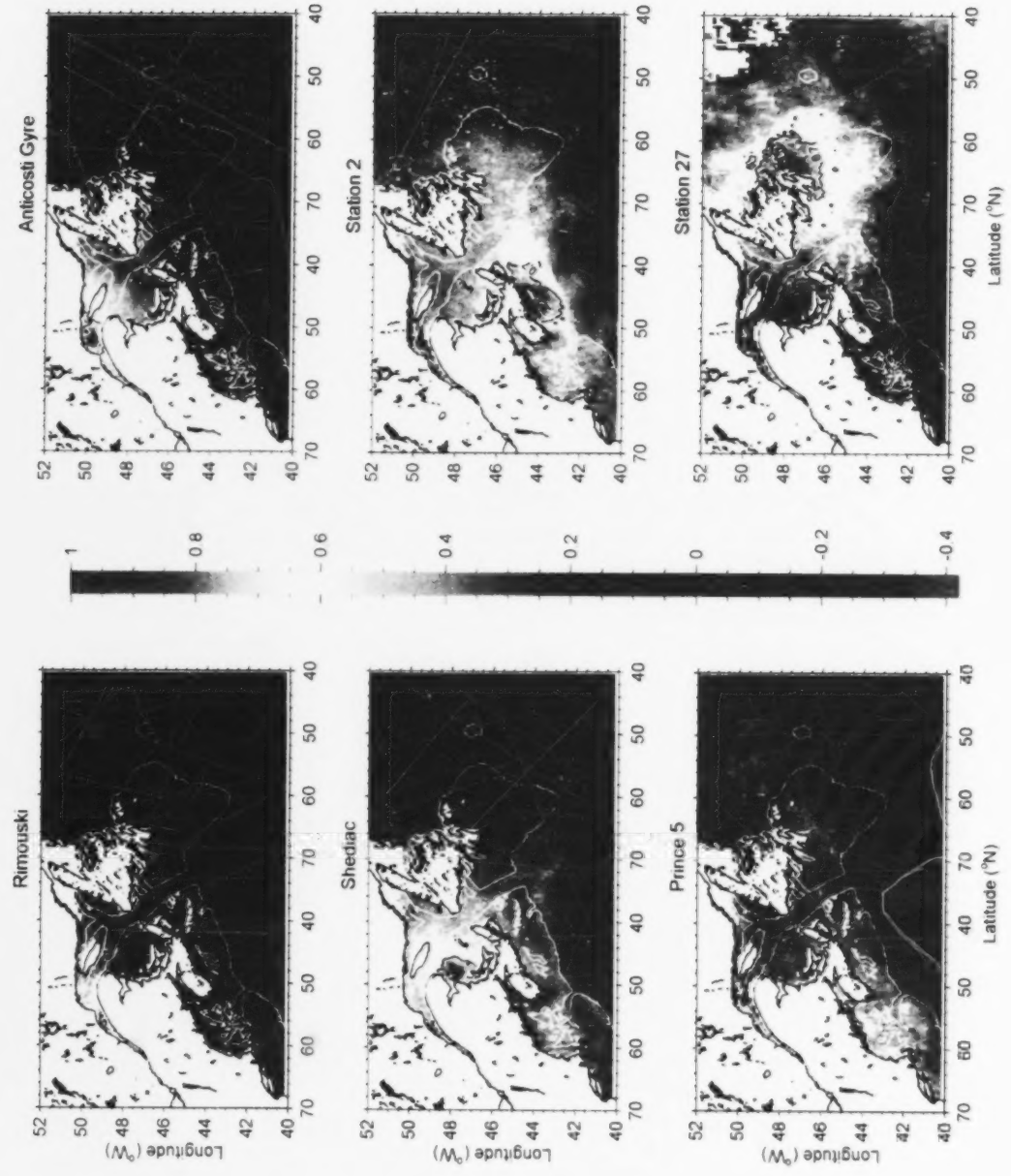

Figure 16. Correlation coefficients relative to pixels near AZMP fixed stations.

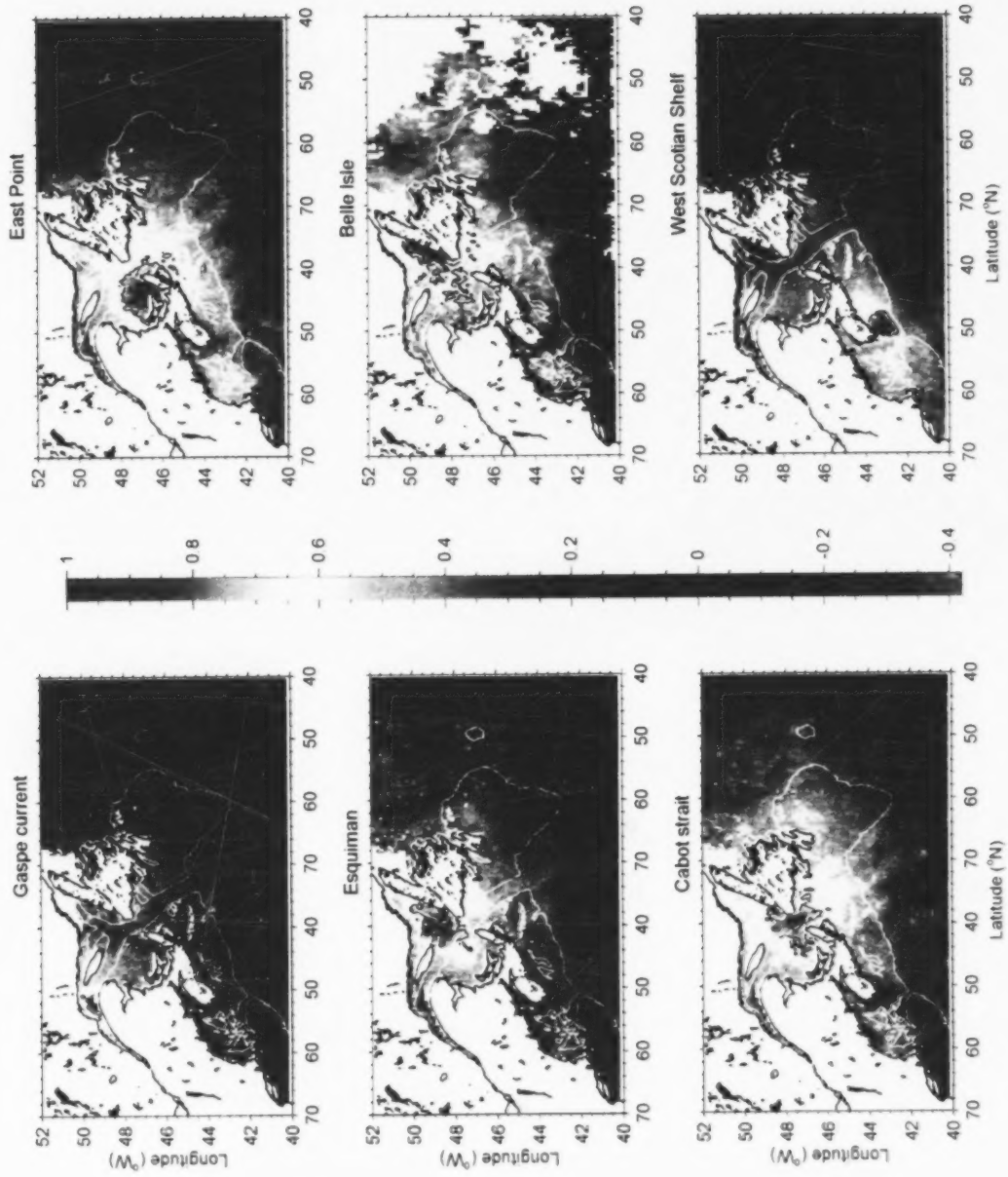

Figure 17. Correlation coefficients relative to Gulf of St. Lawrence and Scotian Shelf locations.

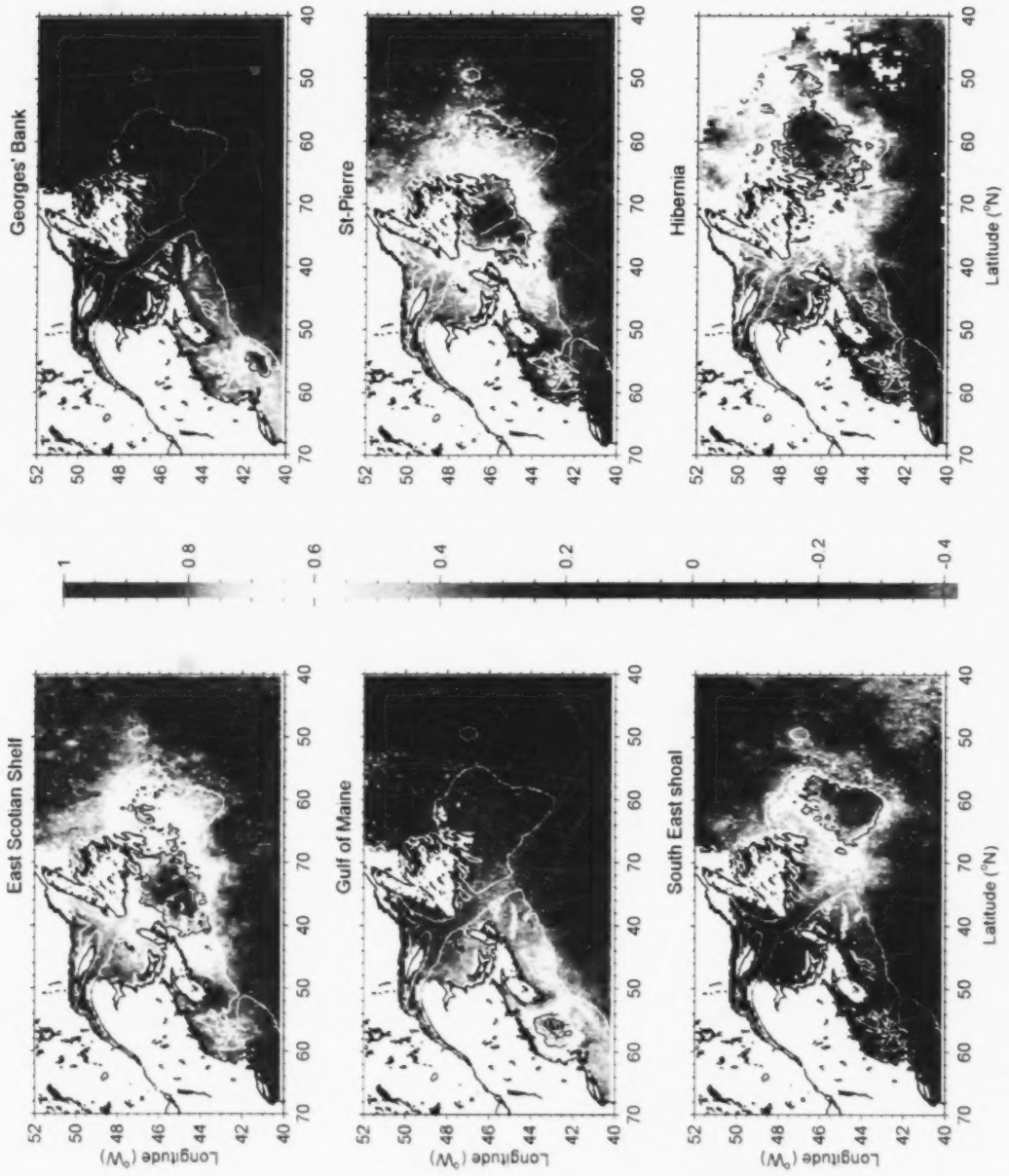

Figure 18. Correlation coefficients relative to pixels in Gulf of Maine and on the Grand Banks.

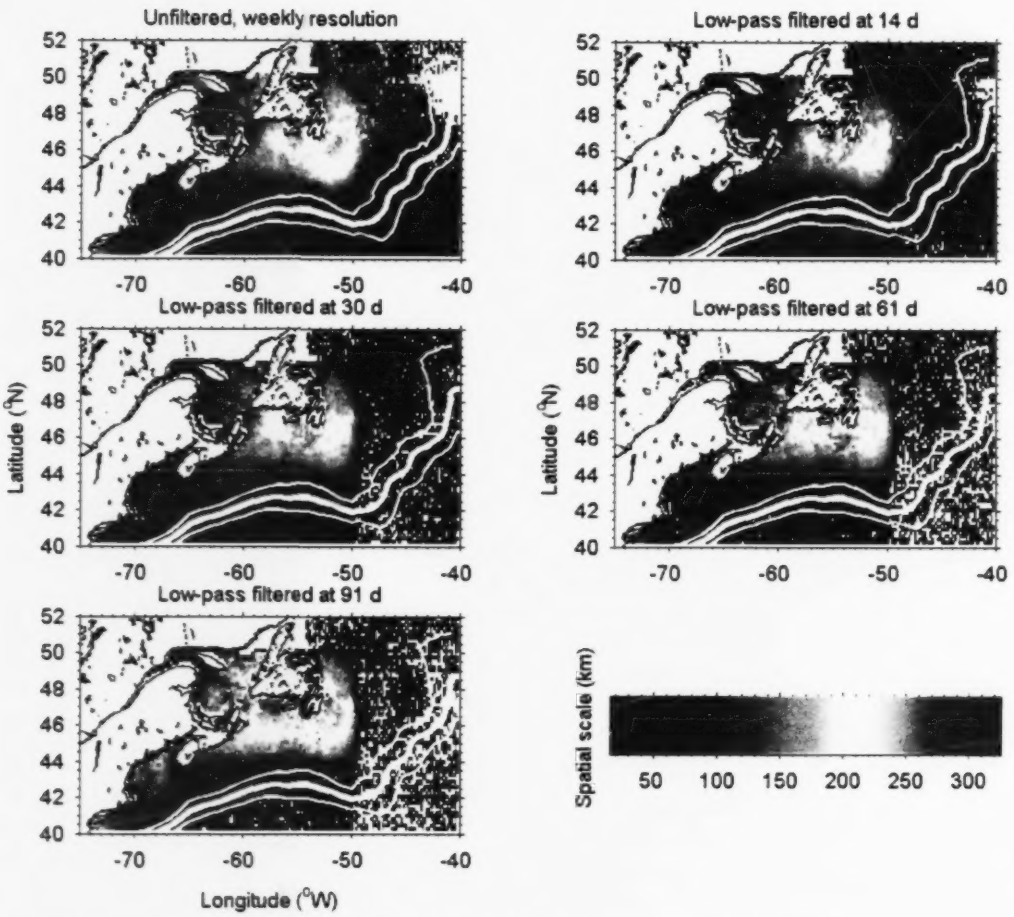

Figure 19. Spatial scales of weekly sampled and filtered (14 d to 91 d) SST anomalies.

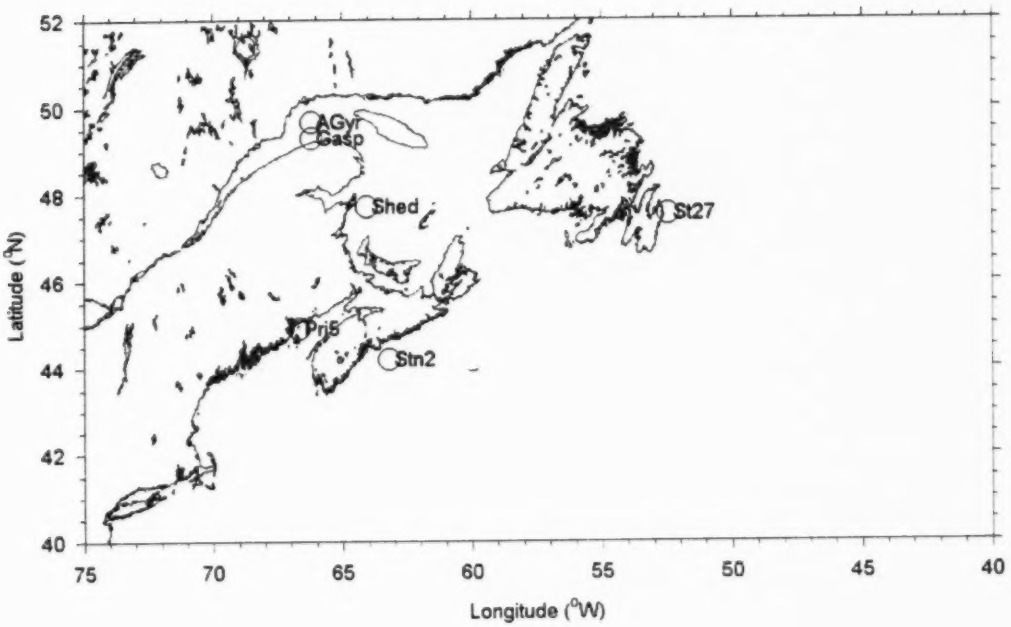

Figure 20. Areas (grey) where AZMP fixed stations cover 50% and more of the SST anomaly variance.

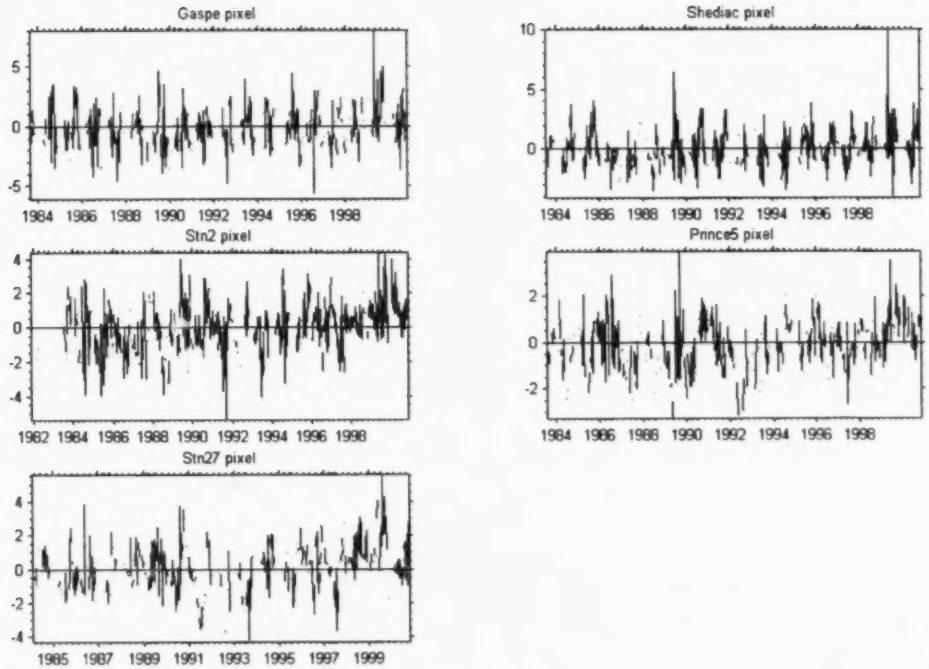

Figure 21. Time series of SST anomalies for 3 by 3 pixel area centred on the AZMP fixed stations.

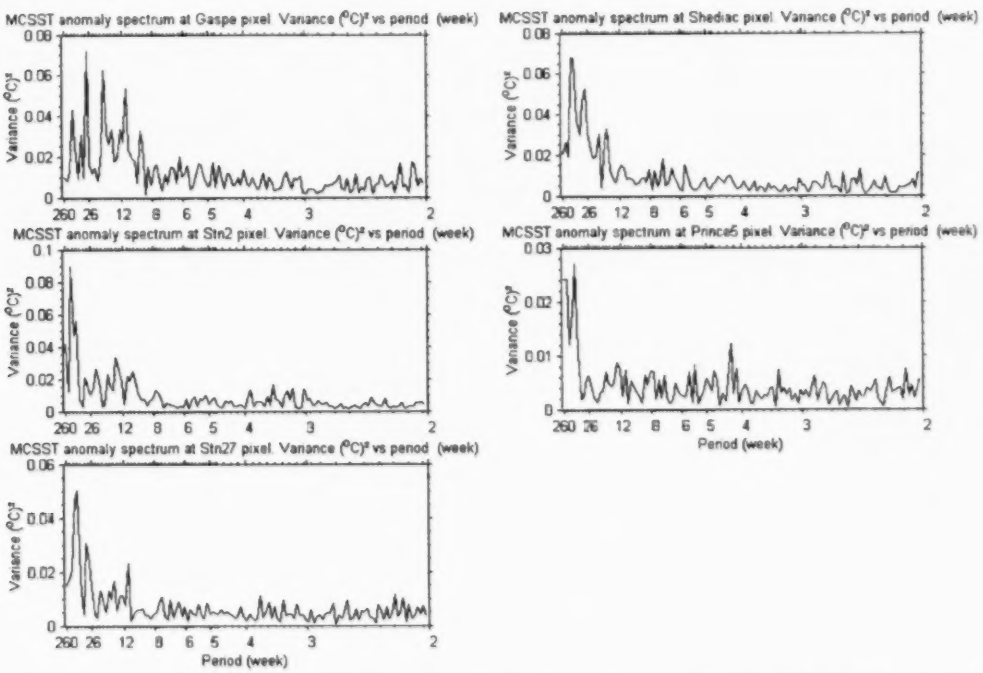
MCSST anomaly spectrum at Gaspe pixel. Variance (°C)² vs period (week)
MCSST anomaly spectrum at Shediac pixel. Variance (°C)² vs period (week)
MCSST anomaly spectrum at Stn2 pixel. Variance (°C)² vs period (week)
MCSST anomaly spectrum at Prince5 pixel. Variance (°C)² vs period (week)
MCSST anomaly spectrum at Stn27 pixel. Variance (°C)² vs period (week)
Variance (°C)²
Period (week)

Figure 22. Spectra of SST anomalies for 3 by 3 pixel area centred on the AZMP fixed stations.

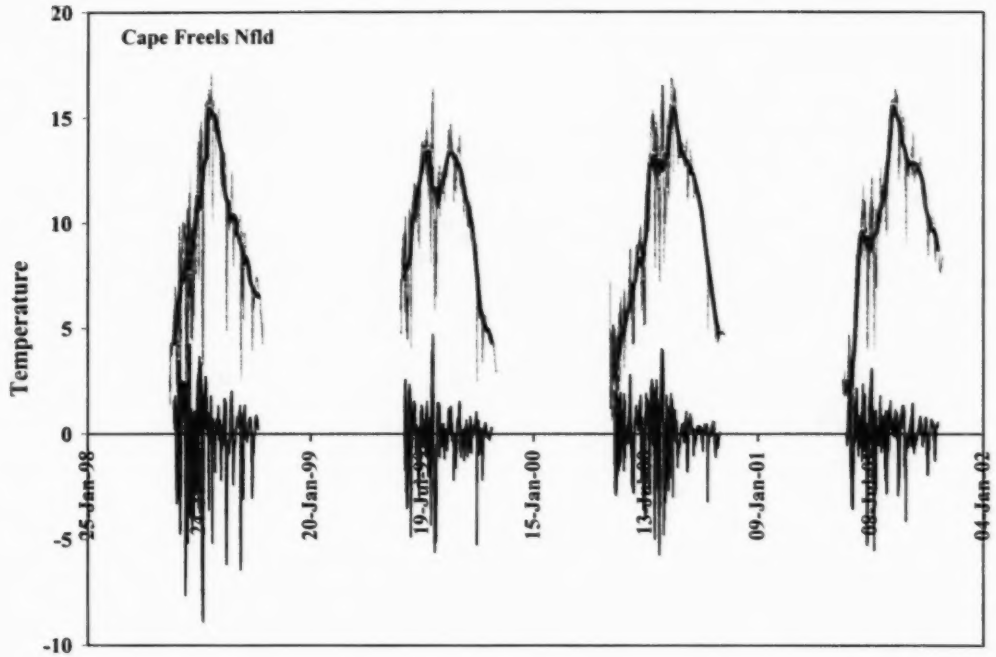

Figure 23. Time series of near-surface temperature at Cape Freels, Newfoundland. The grey line represents the original data, the thick black line the 2 week running mean filter , and the thin black line along the x axis, the difference between the original and filtered data (i.e., the series represented periods less than 2 weeks).

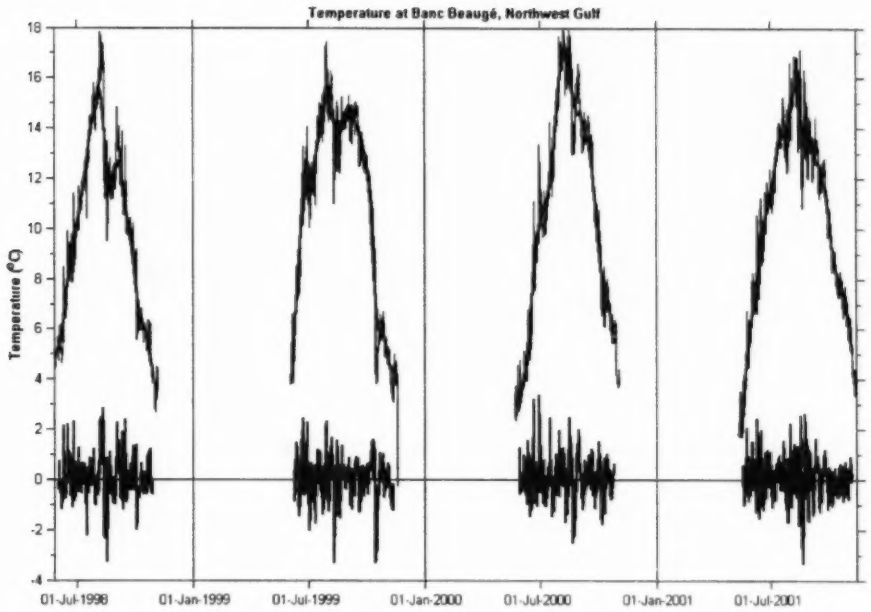

Figure 24. Time series of near-surface temperature at Banc Beaugé, Northeast Gulf of St. Lawrence. The grey line represents the original data, the thick black line the 2 week running mean filter , and the thin black line along the x axis, the difference between the original and filtered data (i.e., the series represented periods less than 2 weeks).

Appendix I

Example of the first method to estimate spatial scales of variability at a given pixel (example shown : 72.686°W and 40.166°N).

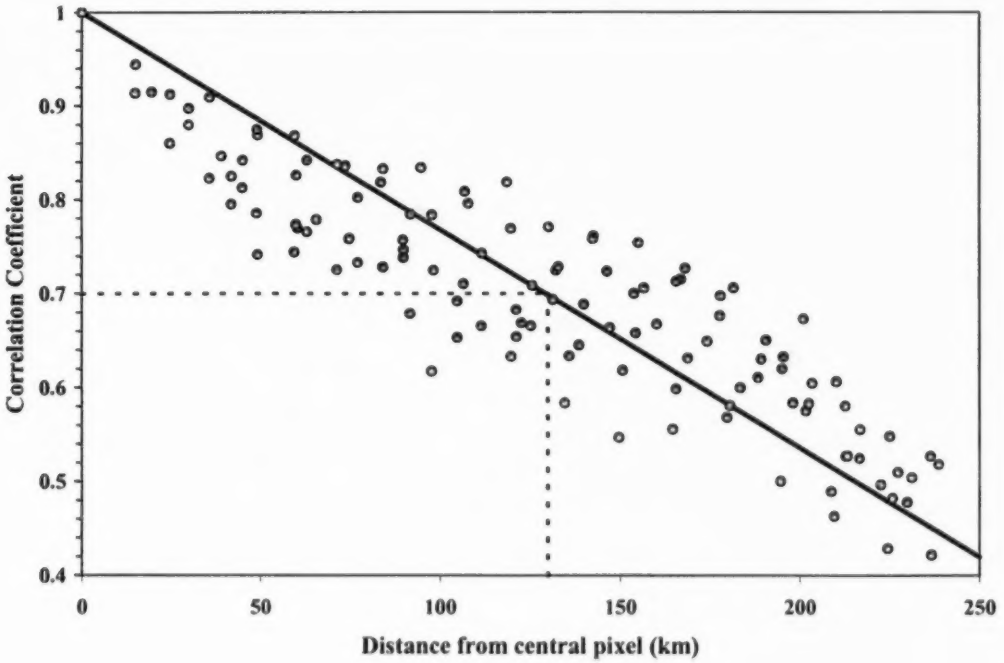

1)Correlation coefficients are sorted by distance from the central pixel (dots)
2)A linear function is least-square fitted (solid line)
3)The 0.7 correlation coefficient intercept (dotted line) is then taken as the spatial scale of variability for each pixel and is independent of the direction from it

In this case, the spatial scale of variability is 130 km.